EXERGY-BASED PERFORMANCE ANALYSIS AND EVALUATION OF A DUAL-DIESEL CYCLE ENGINE

by

Guven GONCA[a*] and Mehmet Fatih HOCAOGLU[b]

[a] Yildiz Technical University, Naval Architecture and Marine Engineering Department, Besiktas, Istanbul, Turkey
[b] Industrial Engineering, Medeniyet University, Istanbul, Turkey

Original scientific paper
https://doi.org/10.2298/TSCI190710180G

Performance examinations of a dual-Diesel cycle engine in point of engine performance characteristics such as exergy efficiency, power and power density have been conducted. The effect of design parameters of the engine cycle such as intake temperature, intake pressure, piston friction coefficient, average piston velocity, engine revolution, stroke length, residual gas fraction, engine pressure ratio, engine temperature ratio, compression ratio, ratio of bore diameter to stroke length, and equivalence ratio, on the performance characteristics are evaluated by considering variable specific heats and irreversibilities resulting from exhaust output, heat transfer, incomplete combustion and friction. The results can provide substantial information researchers who study on dual-Diesel cycle engine design and manufacture.

Key words: *dual-Diesel cycle engine, compression ignition engine, exergy, power density, performance analysis*

Introduction

Gasoline engine and Diesel engine are commonly used in the transportation and energy generation sectors. There are so many optimization works about them and their cycles such as Otto cycle engine (OCE), Diesel cycle engine (DCE), dual-Diesel cycle (DDC) and the other cycles such as Atkinson and Miller cycles which are performed by engine designers to satisfy economical and environmental demands. Chen *et al.* [1] performed an observation describe the cycle work and thermal efficiency relations for an OCE taking energy loss depend on heat transfer (HT) into account. Ge *et al.* [2, 3] conducted a work on the performances of reversible [2] and irreversible [3] OCE soperating on working fluid which has chancing specific heat with respect to temperature variation. Chen *et al.* [4] defined cycle efficiency and power of an OCE with considerations of HT and isentropic loss. Ozsoysal [5] described the losses depending on HT processes with respect to combustion energy of the fuel for DCE and OCE. Ge *et al.* [6] examined the impact of specific heat variation with respect to temperature variation and energy loss arising from friction and HT on the engin performance (EPER) characteristics of an OCE. Abu-Nada *et al.* [7] thermodynamically analyzed the performance of an spark ignition (SI) and OCE using a novel model considering the gas blend effects of the enthalpy variation. Lin and Hou [8] computationally demonstrated the impact of specific heat variation with respect to temperatures, friction and HT loss on the EPER specifications of an OCE under maximum cycle temperature conditions. Ust *et al.* [9] performed an examination on the influences of engine

* Corresponding author, e-mail: ggonca@yildiz.edu.tr

pressure ratio (EPR) and engine temperature ratio (ETR) on the engine work and efficiency of the OCE. Cesur *et al.* [10] performed a work on a steam injected SI and OCE to demonstrate the EPER characteristics and exhaust emission formations. Gharehghani *et al.* [11] performed an experimental study on the EPER characteristics of a turbocharged SI and OCE operating on natural gas. Irimescu *et al.* [12] developed a novel technique for measurement of compression ratio, r, and blow-by rate for an SI engine. Al-Hinti *et al.* [13] proposed a different computation method for HT loss to anal ysis the EPER of a DCE. Hou [14] perused the impact of HT losses on the EPER specifications of a dual-Diesel cycle engine (DDCE). Ust *et al.* [15] enlarged the former work for an irreversible DDCE. Xia *et al.* [16] determined the performance properties of a DCE by considering irreversibilities originating from incomplete combustion (IC) of fuel, friction and HT. Gonca *et al.* [17-22] performed a couple of studies on the Miller cycle Diesel engines [20-24] and steam injected Diesel engines [21-22].

Gharehghani *et al.* [23] asserted that an optimized common-rail DC engine provides higher thermal efficiency and lower exhaust emission formations compared to that without optimization. Acikkalp *et al.* [24] performed an analysis for a gas-Diesel engine tri-generation system using exergetic approach. Ozsoysal [25] exploited the combustion-based efficiency to define IC in a DDCE covering irreversibility arising from processes during the compression and expansion. Acikkalp and Caner [26] researched the performance specifications of a nanoscale DDC using Ideal Maxwell/Boltzmann gas constant. Acikkalp and Caner [27] used and compared different thermodynamic assessment methods to investigate the performance characteristics of a nanoscale DDC working with ideal Fermi and Bose gas constants. Ge *et al.* [28] utilized a finite-time thermodynamics model (FTTM) to investigate the EPER characteristics of the OC, DC, and DDC engines taking friction losses heat losses and internal irreversibilities into consideration. Gonca and Sahin [29] investigated the influences of hydrogen addition into a steam injected Diesel engine. Vellaiyan and Amirthagadeswaran [30] performed a study on the optimization of operating parameter for a Diesel engine fuelled with diesel-water emulsions. Liu *et al.* [31] examined the influences of ethanol-diesel blends, injection timing and exhaust gas re-circulation application on the particulate matter emission and combustion properties of a Diesel engine. Palaci and Gonca [32] investigated the variations of different cylinder materials and equivalence ratios, ϕ, on the performance characteristics of a Diesel engine. Engine researchers also studied on the optimizations of different cycle engines [33-51].

In the presented work, the impacts of each operational and design parameter on the EPER specifications such as power, power density, and exergy efficiency (EXEF) and irreversibilities for an DDC engine have been parametrically studied using a realistic finite-time thermodynamics modeling. Presented results have a scientific value and they can be utilized by DDCE designers to obtain optimized conditions of the performance.

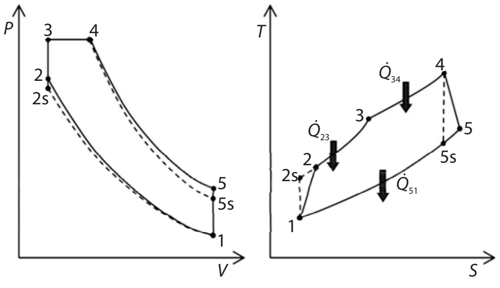

Figure 1. The *P-v* and *T-s* diagrams for the irreversible DDC

Theoretical model

A parametrical and numerical analysis has been carried out to determine power, power density, and EXEF of an DDCE. The *T-s* and *P-v* diagram of the engine cycle is depicted in fig. 1.

In the numerical section, the values in the tab. 1 have been used at the standard conditions. In the presented calculation, the power, power density, and EXEF are obtained:

$$P_O = \dot{Q}_{\text{in}} - \dot{Q}_{\text{out}} - P_{fr}, \quad P_d = \frac{P_O}{V_T}, \quad \varepsilon = \frac{\dot{m}_f \psi_f - \dot{X}_{\text{dest,tot}}}{\dot{m}_f \psi_f} \tag{1}$$

In processes 2-3 and 3-4, heat additions into the cycle are carried out. The $\dot{Q}_{\text{in}}$ is the total heat addition. In process 5-1, heat output from the cycle is carried out, $\dot{Q}_{\text{out}}$ is the total heat output. The $\dot{Q}_{\text{in}}$, $\dot{Q}_{\text{out}}$, and P_{fr} are given:

$$\dot{Q}_{\text{in}} = \dot{Q}_{fc} - \dot{Q}_{ht} = \dot{m}_T \left[\int_{T_2}^{T_3} C_V \mathrm{d}T + \int_{T_3}^{T_4} C_P \mathrm{d}T \right] =$$

$$= \dot{m}_T \left(\begin{aligned} & \left[\begin{aligned} & 2.506 \cdot 10^{-11} \frac{T^3}{3} + 1.454 \cdot 10^{-7} \frac{T^{2.5}}{2.5} - 4.246 \cdot 10^{-7} \frac{T^2}{2} + 3.162 \cdot 10^{-5} \frac{T^{1.5}}{1.5} + \\ & + 1.0433T - 1.512 \cdot 10^4 \left(-\frac{T^{-0.5}}{0.5} \right) + 3.063 \cdot 10^5 \left(-T^{-1} \right) - 2.212 \cdot 10^7 \left(-\frac{T^{-2}}{2} \right) \end{aligned} \right]_{T_2}^{T_3} + \\ & + \left[\begin{aligned} & 2.506 \cdot 10^{-11} \frac{T^3}{3} + 1.454 \cdot 10^{-7} \frac{T^{2.5}}{2.5} - 4.246 \cdot 10^{-7} \frac{T^2}{2} + 3.162 \cdot 10^{-5} \frac{T^{1.5}}{1.5} + \\ & + 1.3301T - 1.512 \cdot 10^4 \left(-\frac{T^{-0.5}}{0.5} \right) + 3.063 \cdot 10^5 \left(-T^{-1} \right) - 2.212 \cdot 10^7 \left(-\frac{T^{-2}}{2} \right) \end{aligned} \right]_{T_3}^{T_4} \end{aligned} \right) \tag{2}$$

$$\dot{Q}_{\text{out}} = \dot{m}_T \int_{T_1}^{T_5} C_V \mathrm{d}T =$$

$$= \left[\dot{m}_T \left(\begin{aligned} & 2.506 \cdot 10^{-11} \frac{T^3}{3} + 1.454 \cdot 10^{-7} \frac{T^{2.5}}{2.5} - 4.246 \cdot 10^{-7} \frac{T^2}{2} + 3.162 \cdot 10^{-5} \frac{T^{1.5}}{1.5} + \\ & + 1.0433T - 1.512 \cdot 10^4 \left(-\frac{T^{-0.5}}{0.5} \right) + 3.063 \cdot 10^5 \left(-T^{-1} \right) - 2.212 \cdot 10^7 \left(-\frac{T^{-2}}{2} \right) \end{aligned} \right) \right]_{T_1}^{T_5} \tag{3}$$

where P_{fr} is friction power [17]:

$$P_{fr} = \mu \bar{S}_P^{\,2} = \frac{\left[Z + 48 \left(\frac{N}{1000} \right) + 0.4 \bar{S}_P^{\,2} \right] V_s N}{1200} \tag{4}$$

$$\dot{m}_T = \dot{m}_a + \dot{m}_f \tag{5}$$

where V_T is total cylinder volume, $\dot{m}_a$ – the air mass-flow rate, $\dot{m}_f$ – the fuel mass-flow rate, ψ_f – the fuel exergy, it is 47137 kJ/kg for Dodecane ($C_{12}H_{26}$) [52], and $\dot{X}_{\text{dest,tot}}$ – the total exergy destruction of the engine cycle per second:

$$\dot{X}_{\text{dest,tot}} = \dot{m}_T \left[T_0 s_{\text{gen,tot}} \right] \tag{6}$$

where $s_{\text{gen,tot}}$ is the total entropy generation per cycle and it is calculated:

$$s_{\text{gen,tot}} = s_{1-2} + s_{2-3} + s_{3-4} + s_{4-5} + s_{5-1} \tag{7}$$

where

$$s_{1-2} = s_2 - s_1 \tag{8}$$

$$s_{2-3} = (s_3 - s_2) - \frac{q_{\text{in},2-3}}{T_{\text{source}}} \tag{9}$$

$$s_{3-4} = (s_4 - s_3) - \frac{q_{\text{in},3-4}}{T_{\text{source}}} \tag{10}$$

$$s_{4-5} = s_5 - s_4 \tag{11}$$

$$s_{5-1} = (s_1 - s_5) + \frac{q_{\text{in},1-5}}{T_{\sin k}} \tag{12}$$

where T_{source} and $T_{\text{sin}k}$ are maximum temperature and ambient temperature, respectively. The other equations have been obtained from [53, 54].

Table 1. Operational and design parameters of the DDCE at the standard conditions

ETR-α	8
Cylinder wall temperature, T_w	400 K
Friction coefficient, μ	12.9 Ns/m
Residual gas fraction, RGF	0.05
Engine speed, N	5000 rpm
Cylinder bore, D	0.072 m
Stroke length, L	0.062 m
Inlet temperature, T_I	300 K
Inlet pressure, P_I	100 kPa

Results and discussion

In the presented work, a simulation model is implemented to a DDCE to assess the power, power density, and EXEF.

Figure 2 demonstrates the effect of ETR on the EPER specifications. The maximum EXEF, power, and power density enhance with rising ETR on account of higher energy transfer into the engine cylinder.

Figure 3 characterizes the impact of N on the EPER characteristics. The power and power density raise with augmenting N. On the other hand, the EXEF is lower at higher speed

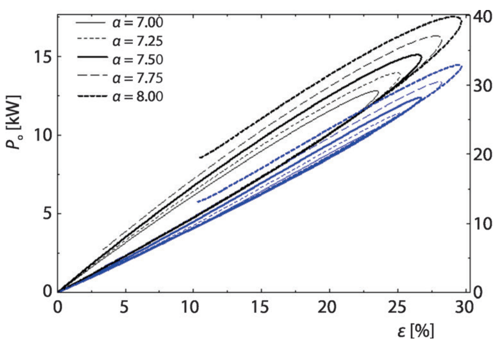

Figure 2. The P_O-P_d-ε against to α

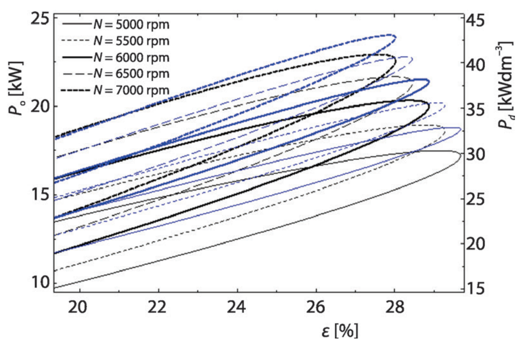

Figure 3. The P_O-P_d-ε against to N

as the irreversibility arising from friction augment with rising speed. The enhancement ratio of fuel energy during the combustion in the cylinder is higher in comparison with that of power and power density, thus EFEF diminishes with increasing engine speed.

Figures 4(a) and 4(b) depict the influence of cycle pressure ratio, λ, and N on the EPER characteristics. It is know in the literature that the λ is a ratio of maximum cycle pressure to minimum cycle pressure. They improve with increasing λ owing to enhancing in-cylinder pressure, temperature, and compression ratio, r. The power and power density enhance with augmenting engine speed. However, the EXEF increases to about 3000 rpm and then it minimizes with increasing engine speed due to maximizing friction losses.

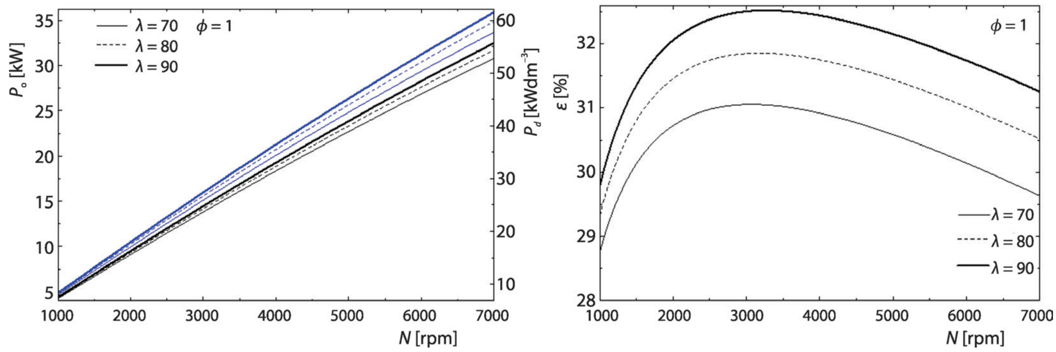

Figure 4. The P_O-P_d-ε against to λ

Figures 5(a) and 5(b) illustrate the effect of linear average piston speed, $\bar{S}_p$, on the EPER characteristics. The performance properties have been evaluated at the conditions of constant speed, fig. 5(a), and constant stroke, fig. 5(b). It has been illustrated that the EPER characteristics augment together with rising $\bar{S}_p$ since the engine dimensions enlarge depending on the enhancement of engine stroke length, L, and bore diameter, D. Whilst the EXEF minimizes, the power, and power density enhance with rising $\bar{S}_p$ on account of raising speed.

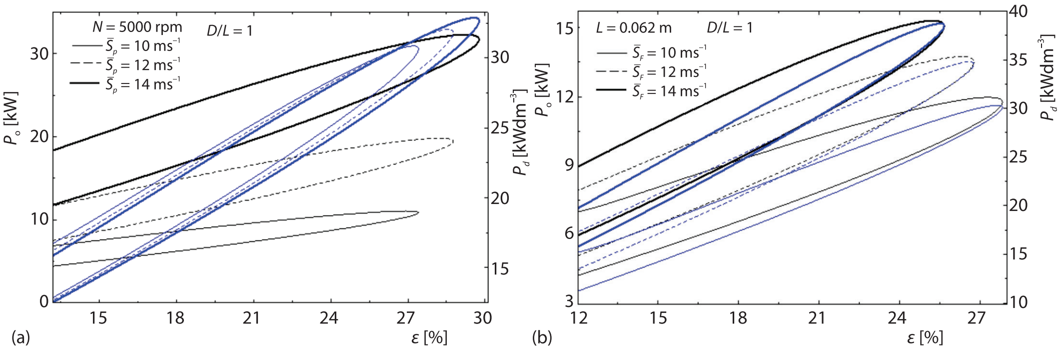

Figure 5. The P_O-P_d-ε against to $\bar{S}_p$ at constant; (a) N and (b) L

Figure 6 indicates the effect of stroke, L, on the EPER properties. The power enhances whilst the EXEF and power density diminish with respect to extending stroke, because the friction losses and the dimension of the engine expand in connection with stroke increment. Even though power enhances, the dimension of the engine more enhances. Thus, the power density minimizes with maximizing power. The change range of the power is larger compared to that of power density.

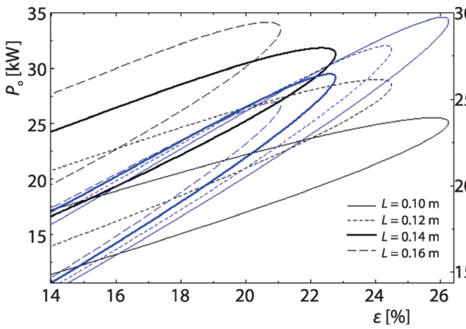

Figure 6. The P_O-P_d-ε against to L

Figures 7(a) and 7(b) depict the impact of air inlet temperature on the EPER characteristics at fixed ETR and constant maximum combustion temperature conditions. A considerable improvement is observed in the EPER properties with enhancing temperature of the inlet air as energy addition into the engine per cycle remarkably rises at the constant ETR condition. The EPER characteristics reduce with enhancing air intake temperature owing to diminishing air mass.

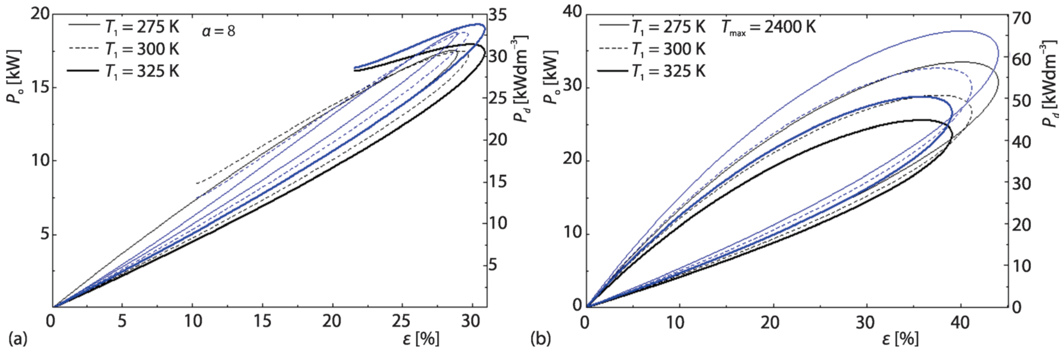

Figure 7. The P_O-P_d-ε against to T_1 at constant; (a) α and (b) $T_{\max}$

Figures 8(a) and 8 (b) indicate the effect of ϕ and γ on the ETR and the EPER specifications. The ETR augments and the EPER improves with enhancing r, nevertheless, they augments to precise points and minimized after the maximum points with respect to enlarging ϕ.

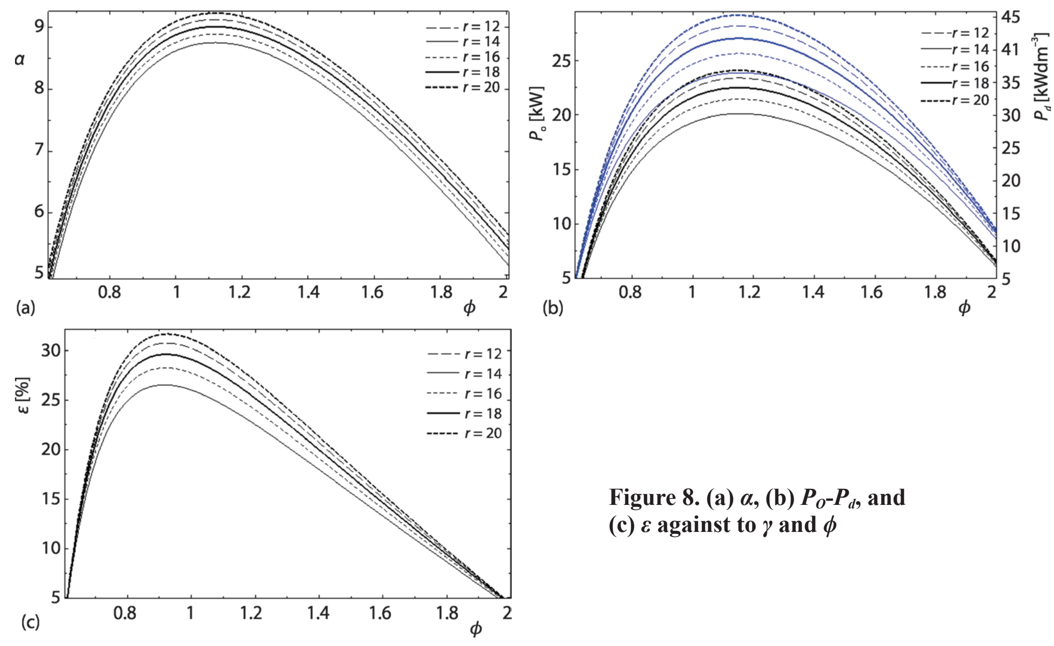

Figure 8. (a) α, (b) P_O-P_d, and (c) ε against to γ and ϕ

These results are similar to those of [53]. It can be said that r and ϕ variations lead to similar results for the engine cycles.

Figure 9 depicts the impact of ϕ on the EPER specifications. As similarly to former figures, the EPER have parabolic specifications. The maximum EXEF is acquired at 1 of ϕ whilst the peak EFPO is attained at 1.2 of it.

Figure 10 illustrates the impact of wall temperature of the cylinder on the EPER characteristics. Remarkable change is not observed in the peak power and power dwnsity relating to the variation of the cylinder wall temperature, nevertheless, the peak EXEF diminishes with minimizing cylinder wall temperature as the energy losses in connection with HT enhance with reducing wall temperature.

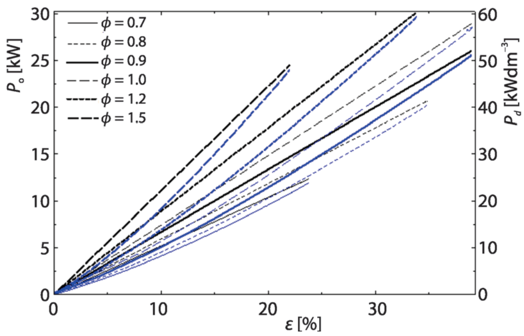

Figure 9. The P_O-P_d-ε against to ϕ

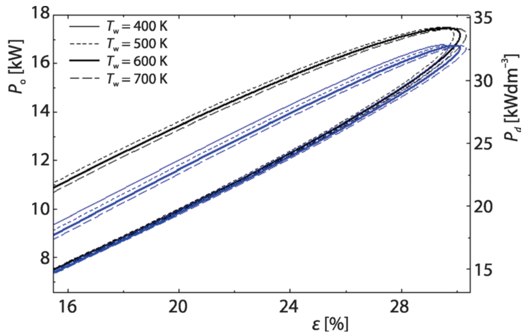

Figure 10. The P_O-P_d-ε against to T_W

Figure 11 displays the impact of inlet pressure, P_1, on the EPER specifications. They enhance with raising air inlet pressure as more air amounts are taken inside the cylinder at higher pressure condition.

The effect of D/L on the EPER specifications are illustrated in fig. 12. The EPER properties improve with expanding D/L by virtue of enlarging engine dimension.

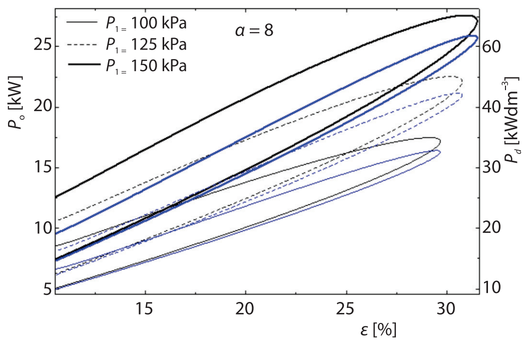

Figure 11. The P_O-P_d-ε against to P

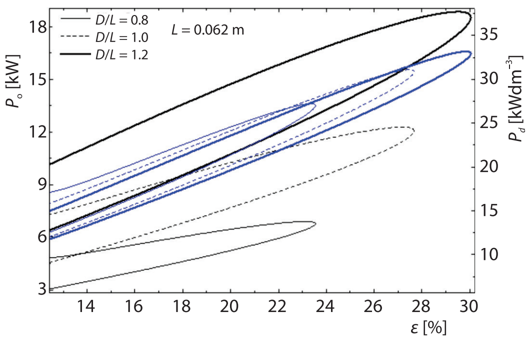

Figure 12. The P_O-P_d-ε against to D/L

Figures 13(a) and 13 (b) depict the impact of D/L on the EPER specifications at three different conditions of the DDCE with constant cylinder volume. The ϕ and L are constant in fig. 13(a). The EPER characteristics enhance with augmenting D/L by virtue of dimension increment. The ϕ and γ are held constant in fig. 13(b). The variation trends of the curves in this figure is similar to previous figure.

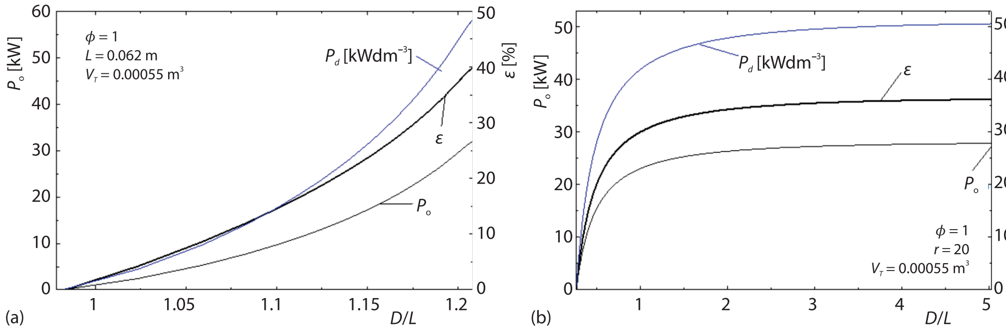

Figure 13. Influence of D/L on P_O-P_d against to at constant; (a) ϕ and L, and (b) ϕ and r

Figures 14(a) and 14(b) exhibit the impact of γ on the energy loss as a percentage of fuel combustion energy at constant ETR and at constant ϕ as two different conditions. In fig. 14(a), the ETR is held fixed. When r increases, the energy losses depending on exhaust energy, L_{EX}, decreases while the irreversibility originating from HT, L_{HT}, and IC, L_{IC}, increase. However, friction dependent loss, L_{fr}, is fixed. The ϕ and V_T change in connection with variation of r. There is a relation between the variation of the L_{IC} and ϕ. The L_{IC} maximizes with enhancing r at constant ERT by virtue of increasing of energy input resulting from fuel combustion. The ϕ is held constant in fig. 14(b). The L_{IC} and L_{fr} are fixed, L_{HT} augments and L_{EX} abates relating to enhancing r. The V_T enhances with enlarging r, thus L_{HT} maximizes. Available net work augments with rising r and hereby L_{EX} diminishes. The L_{fr} changes in connection with L and N variation, thus, L_{fr} is fixed. Because L and N are also constant in fig. 14(b).

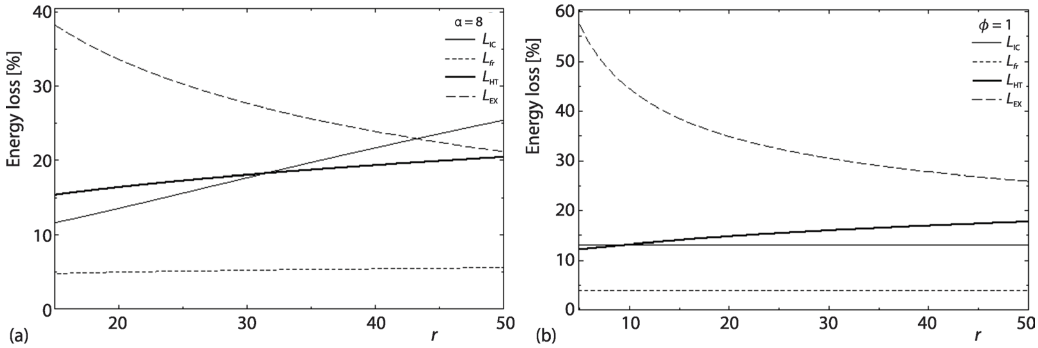

Figure 14. Energy loss percentages against to r for constant; (a) α and (b) ϕ

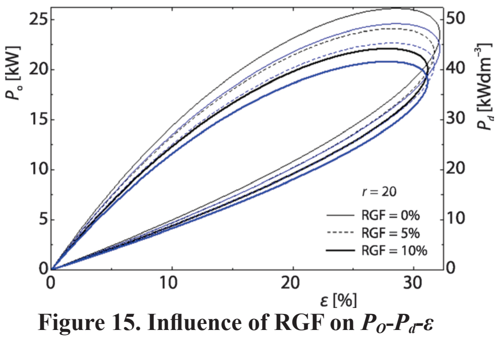

Figure 15. Influence of RGF on P_O-P_d-ε

Figures 15(a) and (15(b) illustrate the impact of RGF on the EPER specifications. The curve trends are similar to each other. The EPER specifications deteriorate with augmenting RGF since air inlet temperature raises and air mass inside the cylinder minimizes with enhancing RGF owing to diminishing density of the working fluid in the engine cylinder.

Conclusion

In this paper, the influence of operating and design parameters of the DDC engine on the EPER characteristics has been examined by computational studies. They improve with enhancing ETR, α, EPR, λ, and air inlet pressure, P_1. The EPER characteristics deteriorate with friction coefficient, μ. However, the power, power density, and EXEF improve with enhancing average piston speed, $\bar{S}_p$, for fixed N circumstances, but while the power and power density increase, the EXEF worsens with increasing average piston velocity for fixed L circumstances. Whilst the power and power density increase, the EXEF diminishes with rising L and N. The power, power density, and EXEF increase by a determined point and then begin to minimize with augmenting r and ϕ. The performance loss enhances in connection with the increment of HT as the irreversibility resulting from IC and exhaust output diminish with enhancing r for the fixed α circumstances. Also, friction loss is held fixed, nevertheless, the loss depending on friction and IC are held fixed, whilst exhaust output-based energetic performance loss diminishes and HT loss augments at the constant ϕ. The results have high scientific value and they can be used by researchers to acquire optimized operating and design conditions for the DDC engines.

References

[1] Chen, L., *et al.,* Heat Transfer Effects on the Net Work Output and Efficiency Characteristics For an Air standard Otto Cycle, *Energ Convers Manage., 39* (1998), 7, pp. 643-648
[2] Ge, Y., *et al.,* Thermodynamic Simulation of Performance of an Otto Cycle with Heat Transfer and Variable Specific heats for the Working Fluid, *Int. J. Therm. Sci., 44* (2005), 5, pp. 506-511
[3] Ge, Y., *et al.,* The Effects of Variable Specific-Heats of the Working Fluid on the Performance of an Irreversible Otto cycle, *Int. J. Exergy, 2* (2005), 3, pp. 274-283
[4] Chen, J., *et al.,* Optimization Criteria for the Important Parameters of an Irreversible Otto Heat-Engine, *Appl. Energy, 83* (2006), 1, pp. 228-238
[5] Ozsoysal, O. A,. Heat Loss as a Percentage of the Fuel's Energy in Air Standard Otto and Diesel Cycles, *Energy Convers. Manage., 47* (2006), 8, pp. 1051-1062
[6] Ge, Y., *et al.,* Finite-Time Thermodynamic Modelling and Analysis of an Irreversible Otto-Cycle. *Appl. Energy, 85* (2008), 7, pp. 618-624
[7] Abu-Nada, E., *et al.,* Thermodynamic Analysis of Spark-Ignition Engine Using a Gas Mixture Model for the Working Fluid. *Int. J. Energy Res., 31* (2007), 1, pp. 1031-146
[8] Lin, J. C., Hou, S. S., Effects of Heat Loss as Percentage of Fuel's Energy, Friction and Variable Specific Heats of Working Fluid on Performance of Air Standart Otto Cycle, *Energy Convers. Manage., 49* (2008), 1, pp. 1218-1227
[9] Ust, Y., *et al.,* The Effects of Cycle Temperature and Cycle Pressure Ratios on the Performance of an Irreversible Otto Cycle, *Acta Phys. Pol. A, 120* (2011),1, pp. 412-416
[10] Cesur, I. *et al.,*The Effects of Electronic Controlled Steam Injection on Spark Ignition Engine, *Appl Therm Eng., 55* (2013), 1, pp. 61-68
[11] Gharehghani, A., *et al.,* Experimental Investigation of Thermal Balance of a Turbocharged SI Engine Operating on Natural Gas, *Appl. Therm. Eng., 60* (2013), 1-2, pp. 200-207
[12] Irimescu, A., *et al.,* Compression Ratio and Blow-by Rates Estimation Based on Motored Pressure Trace Analysis for an Optical Spark Ignition Engine, *Appl. Therm. Eng.*, *61* (2013), 2, pp. 101-109
[13] Al-Hinti, I., *et al.,* Performance Analysis of Air-Standard Diesel Cycle Using an Alternative Irreversible Heat Transfer Approach, *Energy Convers. Manage., 49* (2008), 11, pp. 3301-3304
[14] Hou, S. S., Heat Transfer Effects on the Performance of an Air Standard Dual Cycle, *Energy Conversion and Management*, *45* (2004), 18-19, pp. 3003-3015
[15] Ust, Y., *et al.,* Heat Transfer Effects on the Performance of an Air – Standard Irreversible Dual Cycle, *International Journal of Vehicle Design*, *63* (2013), 1, pp. 102-116
[16] Xia, S., *et al.,* Engine Performance Improved by Controlling Piston Motion: Linear Phenomenological Law System Diesel Cycle, *International Journal of Thermal Sciences, 51* (2012), 1, pp. 163-174
[17] Gonca, G., *et al.,* A Study on Late Intake Valve Closing Miller Cycled Diesel Engine, *Arab. J. Sci. Eng. 38* (2013), 1, pp. 383-393

[18] Gonca, G., *et al.,* Performance Maps for an Air-Standard Irreversible Dual-Miller Cycle (DMC) with Late Inlet Valve cClosing (LIVC) Version, *Energy*, *5* (2013), 1, pp. 285-290
[19] Gonca, G., *et al.,* Investigation of Heat Transfer Influences on Performance of Air-Standard Irreversible Dual-Miller Cycle, *Journal of Thermophysics and Heat Transfer*, *29* (2015), 4, pp. 678-683
[20] Gonca, G., *et al.,* Theoretical and Experimental Investigation of the Miller Cycle Diesel Engine in Terms of Performance and Emission Parameters, *Applied Energy*, *138* (2015), 1, pp. 11-20
[21] Gonca, G., *et al.,* Comparison of Steam Injected Diesel Engine and Miller Cycled Diesel Engine By Using Two Zone Combustion Model, *Journal of the Energy Institute*, *88* (2015), 1, pp. 43-52
[22] Gonca, G., *et al.,* The Effects of Steam Injection on the Performance and Emission Parameters of a Miller Cycle Diesel Engine, *Energy*, *78* (2014), 1, pp. 266-275
[23] Gharehghani, A., *et al.,* Experimental Investigation of Thermal Balance of a Turbocharged SI Engine Operating on Natural Gas, *Appl. Therm. Eng*., *60* (2013), 1, pp. 200-207
[24] Acikkalp, E., *et al.,* Advanced Exergoeconomic Analysis of a Trigeneration System Using a Diesel-Gas Engine, *Applied Thermal Engineering, 67* (2014), 1, pp. 388-395
[25] Ozsoysal, O. A., Effects of Combustion Efficiency on a Dual Cycle, *Energy Conversion and Management*, *50* (2009), 1, pp. 2400-2406
[26] Acikkalp, E., Caner, N., Determining Performance of an Irreversible Nanoscale Dual Cycle Operating with Maxwell-Boltzmann Gas, *Physica A*, *424* (2015), 1, pp. 342-349
[27] Acikkalp, E., Caner, N., Determining of the Optimum Performance of a Nanoscale Irreversible Dual Cycle with Quantum Gases as Working Fluid by Using Different Methods, *Physica A*, *433* (2015), 1, pp. 247-258
[28] Ge, Y*., et al.,* Finite-Time Thermodynamic Modelling and Analysis for an Irreversible Dual Cycle, *Mathematical and Computer Modelling*, *50* (2009), 1, pp. 101-108
[29] Gonca, G., Sahin, B., Simulation of Performance and Nitrogen Oxide Formation of a Hydrogen-Enriched Diesel Engine with the Steam Injection Method, *Thermal Science*, *19* (2015), 6, pp. 1985-1994
[30] Vellaiyan, S., Amirthagadeswaran K. S. N, Multi-Response Optimization of Diesel Engine Operating Parameters Running with Water-in-Diesel Emulsion Fuel, *Thermal Science*, *21* (2017), 1, pp. 427-439
[31] Liu, J., *et al.,* The Effects of EGR and Injection Timing on the Engine Combustion and Particulate Matter Emission Performances Fuelled with Diesel-Ethanol Blends, *Thermal Science*, *22* (2018), 3, pp. 1457-1467
[32] Palaci, Y., Gonca, G., The Effects of Different Engine Material Properties on the Performance of a Diesel Engine at Maximum Combustion Temperatures, *Thermal Science*, *24* (2020), 1A, pp. 183-191
[33] Wu, Z., *et al.,* Power, Eficiency, Ecological Function and Ecological Coefficient of Performance of an Irreversible Dual-Miller Cycle (DMC) with Non-Linear Variable Specific Heat Ratio of Working Fluid, *Eur. Phys. J. Plus*, *132* (2017), 1, 203
[34] Al-Sarkhi, A., *et al.,* Performance Evaluation of Irreversible Miller Engine under Various Specific Heat Models, *Int. Commun. Heat Mass, 34* (2007), 1, pp. 897-906
[35] Al-Sarkhi, A., *et al.,* Efficiency of Atkinson Engine at Maximum Power Density Using Temperature Dependent Specific Heats, *JJMIE*, *2* (2008), 1, pp. 71-75
[36] Yin, Y., *et al.,* Optimal Power and Efficiency of Quantum Stirling Heat Engines, *Eur. Phys. J. Plus*, *132* (2017), 1, 45
[37] Ge, Y*., et al.,* Exergy-Based Ecological Performance of an Irreversible Otto Cycle with Temperature-Linear-Relation Variable Specific Heat of Working Fluid, *Eur. Phys. J*., *132* (2017), 1, 209
[38] Gonca, G., Thermo-Ecological Analysis of Irreversible Dual-Miller Cycle (DMC) Engine Based on the Ecological Coefficient of Performance (ECOP) Criterion, *Iran J. Sci. Technol. Trans. Mech. Eng., 41* (2017), 4, pp. 269-280
[39] Gonca, G., Performance Analysis of an Atkinson Cycle Engine under Effective Power and Effective Power Density Conditions, *Acta Physica Polonica A*, *132* (2017), 4, pp. 1306-1313
[40] Acikkalp, E., Analysis of a Brownian Heat Engine with Ecological Criteria, *Eur. Phys. J. Plus*, *131* (2016), 1, 426
[41] Ebrahimi, R., Effects of Equivalence Ratio and Mean Piston Speed on Performance of an Irreversible Dual Cycle, *Acta Physica Polonica A*, *120* (2011), 3, pp. 384-389
[42] Ebrahimi, R., Effect of Expansion-Compression Ratio on Performance of the Miller Cycle, *Acta Physica Polonica A*, *122* (2012), 4, pp. 645-649
[43] Ebrahimi, R., Performance Analysis of an Irreversible Miller Cycle with Considerations of Relative Air-Fuel Ratio and Stroke Length, *Applied Mathematical Modelling*, *36* (2012), 1, pp. 4073-4079

[44] Ebrahimi, R., Thermodynamic Modelling of an Atkinson Cycle with Respect to Relative Air-Fuel Ratio, Fuel Mass Flow Rate and Residual Gases, *Acta Physica Polonica A*, *124* (2013), 1, pp. 29-34
[45] Ebrahimi, R., Performance Analysis of an Irreversible Miller Cycle with Considerations of Relative Air-fuel Ratio and Stroke Length, *Applied Mathematical Modelling*, *36* (2012), 1, pp. 4073-4079
[46] Xia, S., Chen, L., Capital Dissipation Minimization for a Class of Complex Irreversible Resource Exchange Processes, *Eur. Phys. J. Plus*, *132* (2017), 1, 201
[47] Shadloo, M. S., *et al*., A New and Efficient Mechanism for Spark Ignition Engines, *Energy Convers Manage*., *96* (2015), 1, pp. 418-429
[48] Xia, S., *et al*., Maximum Cycle Work Output Optimization for Generalized Radiative Law Otto Cycle Engines, *Eur. Phys. J. Plus*, *131* (2016), 1, 394
[49] Chen, L., *et al*., Thermodynamic Performance Optimization for an Irreversible Vacuum Thermionic Generator, *Eur. Phys. J. Plus*, *132* (2017), 1, 293
[50] Xia, S., Chen, L., Theoretical and Experimental Investigation of Optimal Capacitor Charging Process in RC Circuit, *Eur. Phys. J. Plus*, *132* (2017), 1, 235
[51] Mousapour, A., *et al*., Performance Evaluation of an Irreversible Miller Cycle Comparing FTT (Finite-Time Thermodynamics) Analysis and ANN (Artificial Neural Network) Prediction, *Energy*, *94* (2016), 1, pp. 100-109
[52] ***, http://www.exergy.se/ftp/exergetics.pdf
[53] Gonca, G., Thermodynamic Analysis and Performance Maps for the Irreversible Dual-Atkinson Cycle Engine (DACE) with Considerations of Temperature-Dependent Specific Heats, Heat Transfer and Friction Losses, *Energy Conversion and Management*, *111* (2016), 1, pp. 205-216
[54] Gonca, G., Hocaoglu F. M., Performance Analysis and Simulation of a Diesel-Miller Cycle (DiMC) Engine, *Arabian Journal for Science and Engineering*, *44* (2019), 6, pp. 5811-5824

Paper submitted: July 20, 2019
Paper revised: March 9, 2020
Paper accepted: May 31, 2020